

ORBITAL MIGRATION OF LOW-MASS PLANETS IN EVOLUTIONARY RADIATIVE MODELS: AVOIDING CATASTROPHIC INFALL

WLADIMIR LYRA¹, SIJME-JAN PAARDEKOOPER², AND MORDECAI-MARK MAC LOW¹

¹ Department of Astrophysics, American Museum of Natural History, 79th Street at Central Park West, New York, NY 10024, USA;
wlyra@amnh.org, mordecai@amnh.org

² Department of Applied Mathematics and Theoretical Physics, University of Cambridge, Wilberforce Road, Cambridge CB3 0WA, UK
 Received 2009 December 25; accepted 2010 March 30; published 2010 May 4

ABSTRACT

Outward migration of low-mass planets has recently been shown to be a possibility in non-barotropic disks. We examine the consequences of this result in evolutionary models of protoplanetary disks. Planet migration occurs toward equilibrium radii with zero torque. These radii themselves migrate inwards because of viscous accretion and photoevaporation. We show that as the surface density and temperature fall the planet orbital migration and disk depletion timescales eventually become comparable, with the precise timing depending on the mass of the planet. When this occurs, the planet decouples from the equilibrium radius. At this time, however, the gas surface density is already too low to drive substantial further migration. A higher mass planet, of $10 M_{\oplus}$, can open a gap during the late evolution of the disk, and stops migrating. Low-mass planets, with 1 or $0.1 M_{\oplus}$, released beyond 1 AU in our models avoid migrating into the star. Our results provide support for the reduced migration rates adopted in recent planet population synthesis models.

Key words: accretion, accretion disks – hydrodynamics – methods: numerical – planet–disk interactions – protoplanetary disks – radiation mechanisms: general

1. INTRODUCTION

The origin of planetary systems remains a major challenge to astrophysical theory. Aside from the quandary of planet formation, planet survival is also a problem. Planet formation occurs when the gas disk is still present, and by exchanging angular momentum with the gas, planets start to migrate. This occurs as the planet excites perturbations in the disk that, in turn, exert torques on the planet. The asymmetry of these perturbations on either side of the planet determines the strength of the torques, and thus the direction of migration.

The main components of the excited perturbations are the one-armed spirals launched at the Lindblad resonances and the librating material on horseshoe orbits in the planet’s corotation region. For low-mass planets, with weak wakes, both the shape of the spiral wake and the resulting Lindblad torque can be treated by linear analysis under some assumptions, particularly of local isothermality. The analytical prediction (Goldreich & Tremaine 1979; Ward 1997; Tanaka et al. 2002), confirmed by numerical simulations (Nelson et al. 2000; D’Angelo et al. 2002; Bate et al. 2003), is that the inner Lindblad resonances lead to positive torques, whereas the outer ones lead to negative torques. The outer Lindblad resonances lie closer to the planet, and thus produce stronger torques, so the planet migrates inwards. This migration mode, referred to as Type I migration, occurs on timescales between 10^4 and 10^5 yr. This is a serious problem for planet formation since these timescales are much shorter than the lifetimes of disks (10^6 – 10^7 yr). Halting or slowing Type I migration is imperative if planets are to survive at all. Indeed, planet population synthesis models (e.g., Alibert et al. 2004; Mordasini et al. 2009) have to assume a reduction factor for Type I migration of 30–1000 in order to match the observed distribution of planetary semimajor axes.

Paardekooper & Mellema (2006) made a major step toward the solution of this problem. They found that when the locally isothermal approximation usually assumed in the literature was

relaxed, the planets migrated outwards. This behavior was explained by Baruteau & Masset (2008) and Paardekooper & Papaloizou (2008) as resulting from an entropy-related torque exerted by material on horseshoe orbits in the corotation region. This mechanism operates in regions of the disk that have a negative entropy gradient and inefficient radiative cooling, where sustenance of the torque requires some viscous and thermal diffusion (Paardekooper & Papaloizou 2008). Kley & Crida (2008) and Kley et al. (2009) showed that outward migration indeed occurs in disks with realistic heating and cooling.

This outward migration remains rapid. Planets migrate toward the outer disk, reach an equilibrium radius of zero torque, and stay put thereafter. As emphasized by Paardekooper et al. (2010), slow inward migration then occurs as disk evolution shifts the equilibrium radius inwards. The situation becomes similar to that of gap-opening planets (Type II migration), with the planet migrating in lockstep with the gas as the gas accretes.

This scenario poses a subtle problem that we examine in this Letter. If the planet is moving together with the gas as the disk depletes, at some point in the evolution the disk may reach a thermodynamic state such that inward migration resumes. This brings the problem back to square one, because, if the planet is to survive, the remaining disk lifetime must be shorter than the Type I migration timescale in that evolutionary state. We examine this possibility using one-dimensional evolutionary models of protoplanetary disks including heating and cooling. We describe the model in the following section, present our results in Section 3, and give concluding remarks in Section 4.

2. THE MODEL

2.1. Gas Evolution

We consider non-irradiated disks evolving by viscous diffusion and photoevaporation (Lynden-Bell & Pringle 1974; Lin &

Papaloizou 1979),

$$\frac{\partial \Sigma}{\partial t} = \frac{3}{r} \frac{\partial}{\partial r} \left[r^{1/2} \frac{\partial \Sigma \nu r^{1/2}}{\partial r} \right] - \dot{\Sigma}_w(r, t), \quad (1)$$

where Σ is the surface density, r is the radius, and ν is the effective viscosity. We take the photoevaporation rate to be (Veras & Armitage 2004; Mordasini et al. 2009)

$$\dot{\Sigma}_w = \begin{cases} 0, & \text{for } r < R_g \\ \dot{M}_w / [2\pi(r_{\text{ext}} - R_g)r], & \text{for } r \geq R_g, \end{cases} \quad (2)$$

which is valid for external irradiation.

For temperature evolution, we use a model without shock heating (Nakamoto & Nakagawa 1994)

$$2\sigma T^4 = \tau_{\text{eff}} \left(\frac{9}{4} \Sigma \nu \Omega^2 \right) + 2\sigma T_b^4, \quad (3)$$

where T and T_b are the midplane and background temperatures, respectively, Ω is the Keplerian frequency, and σ is the Stefan–Boltzmann constant. We take the effective optical depth at the midplane (Hubeny 1990; Kley & Crida 2008):

$$\tau_{\text{eff}} = \frac{3\tau}{8} + \frac{\sqrt{3}}{4} + \frac{1}{4\tau}. \quad (4)$$

Equation (3) states that the emerging flux is the result of an equilibrium between viscous heating, background radiation, and radiative cooling. The optical depth is $\tau = \kappa \Sigma / 2$, and the opacities κ are taken from Bell et al. (1997). We assume that although dust growth and planet formation lock away refractory material, fragmentation efficiently replenishes small grains, keeping the disks opaque during their evolution (Birnstiel et al. 2009).

2.2. Planet Evolution

The planet’s orbital radius evolves as

$$\frac{dr_p}{dt} = \frac{2\Gamma}{m_p r_p \Omega_p}, \quad (5)$$

where m_p is the planet’s mass and Γ is the torque from the gas. We assume a circular orbit and constant planet mass. We only consider low-mass planets, and so can ignore the back reaction of the planet onto the gas (Alexander et al. 2006). The torques are modeled with analytical fits valid for the fully unsaturated case (Paardekooper et al. 2010). Using $b/h = 0.4$, where h is the disk’s aspect ratio and b is the gravitational softening of the planet’s potential (necessary in models with less than three dimensions), the torques are

$$\Gamma_{\text{iso}}/\Gamma_0 = -0.85 - \alpha - 0.9\beta, \quad (6)$$

$$\gamma \Gamma_{\text{ad}}/\Gamma_0 = -0.85 - \alpha - 1.7\beta + 7.9\xi/\gamma \quad (7)$$

for the locally isothermal and adiabatic equations of state, respectively. The adiabatic index $\gamma = 1.4$, and α , β , and ξ are the negative of the local density, temperature, and entropy gradients:

$$\alpha = -\frac{\partial \ln \Sigma}{\partial \ln r}; \quad \beta = -\frac{\partial \ln T}{\partial \ln r}; \quad \xi = \beta - (\gamma - 1)\alpha. \quad (8)$$

The torques are normalized by

$$\Gamma_0 = (q/h)^2 \Sigma_p r_p^4 \Omega_p^2, \quad (9)$$

where q is the ratio of planetary to stellar mass and Σ_p is the surface density at the position of the planet. We interpolate between the two torque regimes to get

$$\Gamma = \frac{\Gamma_{\text{ad}} \Theta^2 + \Gamma_{\text{iso}}}{(\Theta + 1)^2}. \quad (10)$$

Here, $\Theta = t_{\text{rad}}/t_{\text{dyn}}$, where t_{rad} and t_{dyn} are the radiative and dynamical timescales. If $\Theta \ll 1$, radiative processes can restore the temperature quickly compared to the horseshoe turnover time, leading to isothermal horseshoe turns. It was shown in Paardekooper & Papaloizou (2009) that the timescale to establish the full horseshoe drag (t_{drag}) is a fraction of the libration timescale (typically $10 t_{\text{dyn}}$ for a $5 M_{\oplus}$ planet). However, as long as $t_{\text{rad}} > t_{\text{dyn}}$, the torque is affected by nonlinear effects, and since the nonlinear torque is so much stronger than its linear counterpart (Paardekooper et al. 2010), the parameter governing linearity (and therefore isothermality) is Θ rather than $t_{\text{rad}}/t_{\text{drag}}$.

Since t_{drag} depends on q , using t_{drag} would lead to different migration behavior for different planet masses. In practice, the transition between isothermal and adiabatic regions occurs on such a small length scale that this would not change the qualitative outcome of the models. Mass segregation is more likely to come from effects of saturation, which we do not consider in this Letter, since it is as yet poorly understood for non-barotropic disks. We note, however, that for viscously heated, optically thick disks close to thermal equilibrium, radiative thermal diffusion will approach the viscous heating rate. Therefore, even in the very optically thick inner regions of the disk, a sizeable fraction of the unsaturated torque can be sustained as long as the disk remains viscous.

To calculate Θ , we consider $t_{\text{rad}} = E/\dot{E}$, where E is the internal energy. The cooling $\dot{E} = \nabla \cdot \mathbf{F}$, where \mathbf{F} is the flux. Using $E = c_v \rho T$, $\rho = \Sigma/2H$, and $|\mathbf{F}| = \sigma T_{\text{eff}}^4$, we have

$$t_{\text{rad}} = \frac{c_v \Sigma \tau_{\text{eff}}}{6\sigma T^3}. \quad (11)$$

The dynamical time $t_{\text{dyn}} = 2\pi/\Omega$, so

$$\Theta = \frac{c_v \Sigma \Omega \tau_{\text{eff}}}{12\pi \sigma T^3}. \quad (12)$$

2.3. Simulation Parameters

We use a one-dimensional linear grid covering 0.1–30 AU with 200 points. The surface density is specified by the initial mass accretion rate \dot{M}_0 , and the viscosity parameter α_{SS} (Shakura & Sunyaev 1973), following the analytical fits of Papaloizou & Terquem (1999) for Σ – ν relations. We use $\dot{M}_0 = 10^{-7} M_{\odot} \text{ yr}^{-1}$ and $\alpha_{\text{SS}} = 10^{-2}$. The wind is modeled with $\dot{M}_w = 10^{-8} M_{\odot} \text{ yr}^{-1}$ and $R_g = 5 \text{ AU}$. For a given surface density, Equation (3) specifies the temperature, with $T_b = 10 \text{ K}$. Because the optical depth depends on temperature, we solve Equation (3) with a Newton–Raphson root-finding algorithm (using 0.01 K precision). We examine planets of mass 0.1, 1, and $10 M_{\oplus}$. Planet–planet interactions are ignored. Boundary conditions are taken as outflow. We compute the derivatives as in the PENCIL CODE,³ with sixth-order spatial derivatives and a third-order Runge–Kutta time integrator.

³ See <http://www.nordita.org/software/pencil-code>

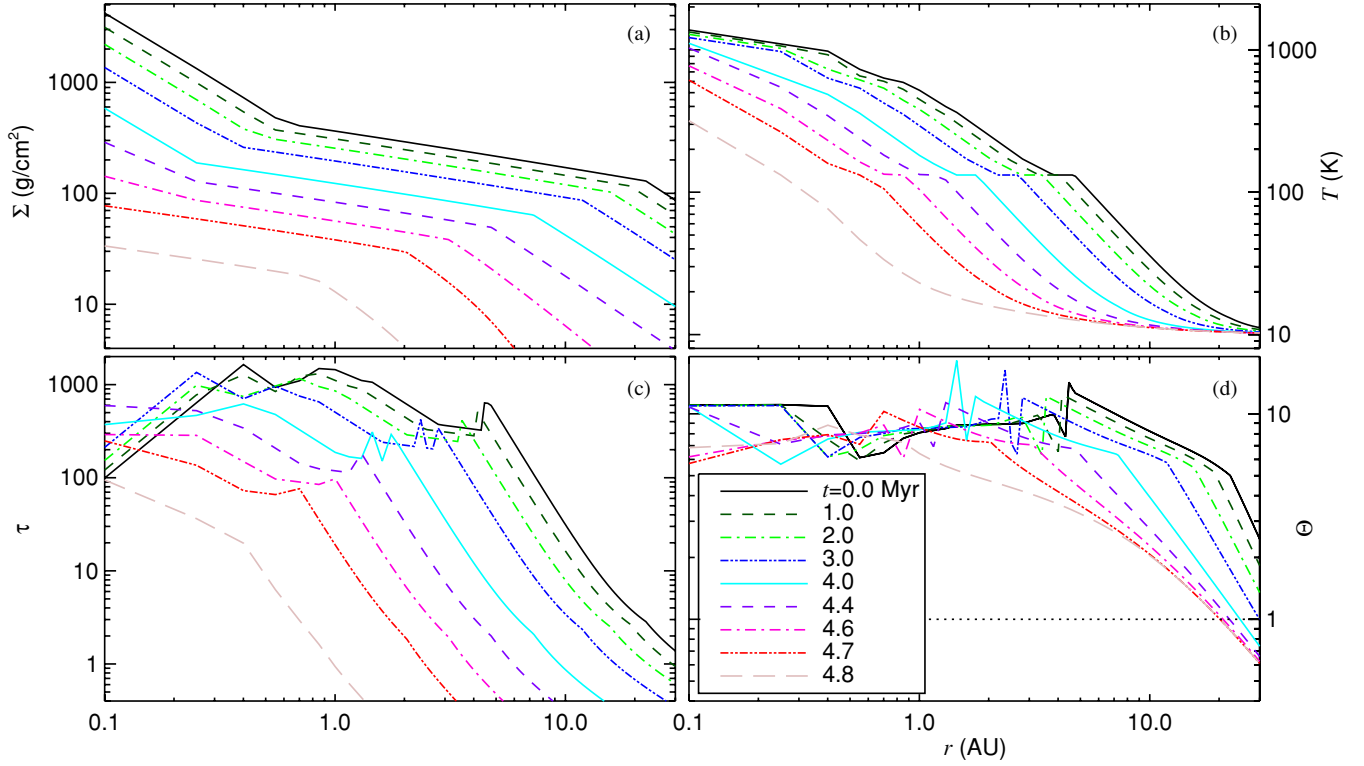


Figure 1. Evolution of (a) surface density, (b) midplane temperature, (c) optical depth, and (d) Θ , the ratio of radiative to dynamical timescales. The disk is drained after 4.8 Myr, with mass dropping below M_{\oplus} . The temperature shows a plateau at ≈ 130 K, produced by the opacity transition when ice grains sublimate that moves inward as the disk cools. Through most of the evolution, $\Theta > 1$, so torques are adiabatic.

3. RESULTS

Figure 1 shows the evolution of our fiducial disk model. The changes in density slope initially located at ~ 0.4 and 21 AU correspond to opacity transitions (Papaloizou & Terquem 1999). The constant temperature plateau initially at 4–5 AU corresponds to the opacity transition at ~ 130 K where ice grains sublimate (see Figure 1(c)). Initially, the ratio of radiative to dynamical timescales $\Theta > 1$ through most of the disk ($\Theta < 1$ only at $r > 70$ AU, beyond the model grid). Thus, the torque in Equation (10) is mostly adiabatic, and largely independent of the interpolation procedure.

Total disk mass and accretion rate decay nearly linearly with time. A disk of $0.08 M_{\odot}$ initially accreting at $10^{-7} M_{\odot} \text{ yr}^{-1}$ gets depleted in 4.8 Myr. At that time, the total disk mass is $< 1 M_{\oplus}$, and we terminate the simulation. The model gives a power-law decline of the density. An inner hole (Clarke et al. 2001) never forms, because of the shallow radial slope of unity for the wind driven by external photoevaporation.

As the surface density drops, so does the viscous heating rate (Equation (3)), and the temperature falls accordingly, down to $T = T_b$. During the evolution, the isothermal plateau shifts inwards from 4 AU to 1 AU by 4.5 Myr. The optical depth only drops to unity at 10 AU after 4 Myr, and at 5 AU after 4.4 Myr, so the planet formation region is optically thick through most of the disk evolution. To check our method, we also ran models with Equation (3), and models where the temperature was derived using (1+1)-dimensional models, following Papaloizou & Terquem (1999). The differences were minor, consisting of a slightly larger isothermal plateau (extending to 6 AU instead of 5 AU), and an outer disk ~ 10 K hotter.

To understand our results for planet migration in evolving disks, we first examine the behavior of planets in stationary

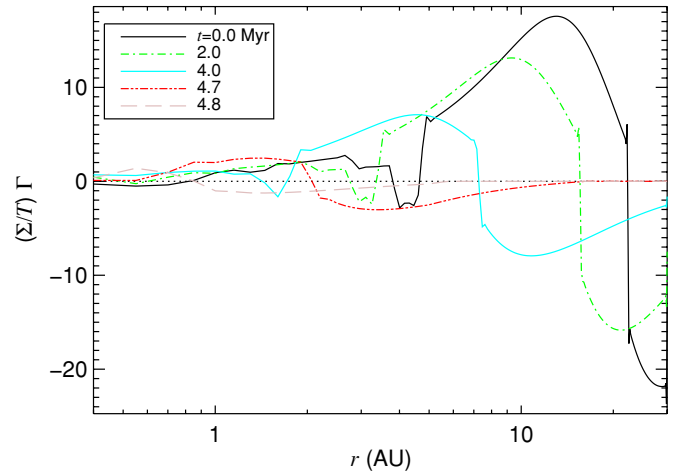


Figure 2. Radial distribution of torque over time (Equation (10)). Positive torques drive outward migration. The equilibrium radii of zero torque shift inwards as the disk evolves. The isothermal plateau corresponds to the well of negative torques initially at 4–5 AU. Discontinuities correspond to opacity jumps. Torques are scaled by Σ/T to aid visualization.

models. In Figure 2, we show the torque as a function of radius. Migration halts at stable equilibrium radii where $\Gamma = 0$ and $d\Gamma/dr < 0$, that is, where the torque is positive within (corresponding to outward migration) and negative outside (inward migration). Two such equilibrium radii occur, at 4 AU and 21 AU, corresponding to the inner boundaries of the isothermal plateau and the outer isothermal region, where $T = T_b$. (There is also a thin region around an equilibrium radius at 0.6 AU that we do not consider here.) A negative torque acts on planets migrating from $r_p > 21$ AU, bringing

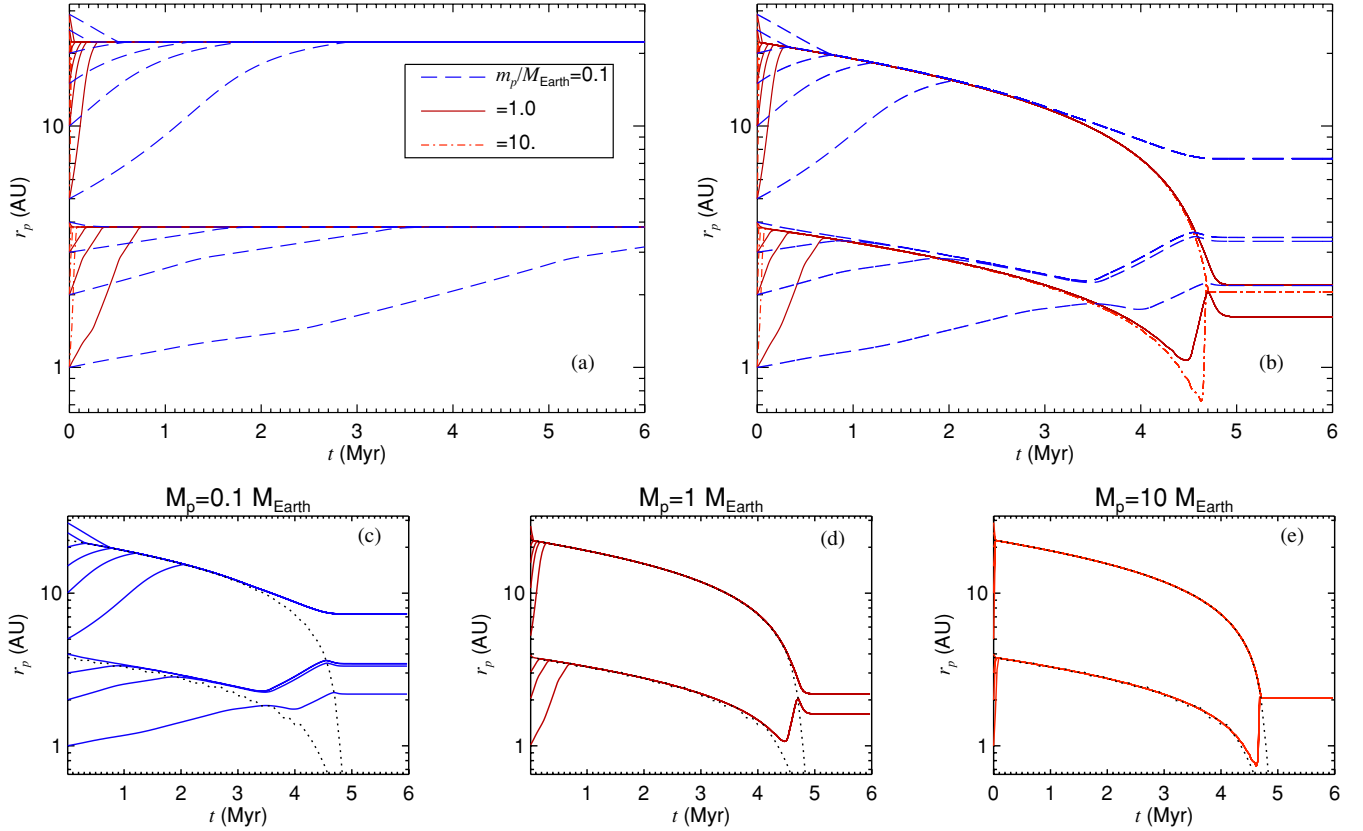


Figure 3. (a) Orbital migration in stationary disks. Planets migrate at mass-dependent rates toward equilibrium radii of zero torque (see Figure 2). (b) Orbital migration in evolving disks. Equilibrium radii migrate inwards on the accretion timescale, but the planets eventually migrate too slowly to remain in equilibrium. In the lower panels (c)–(e) we show the same as in panel (b) but separated by planet mass. The tracks of the equilibrium radii (dotted lines) are shown for comparison.

them to that radius, while a positive torque acts on planets with $4 < r_p/\text{AU} < 21$, also bringing them to that radius. Planets with $r_p < 4$ AU migrate to the inner equilibrium radius.

We released planets of varying mass at several radii in the disk, and see precisely this behavior (Figure 3(a)). The migration time to the equilibrium radius is inversely proportional to the planet mass, because the torque depends quadratically on mass (Equation (9)), so $\dot{r}_p \propto 1/m_p$ (Equation (5)). Planets of $10 M_\oplus$ reach the equilibrium radii in ≤ 0.1 Myr. In the isothermal case, planets migrate inwards at comparable speeds.

In Figure 3(b), we show trajectories of planet migration in an evolving disk. Now the radii of zero torque shift inwards as the disk evolves. The planets migrate to these radii on the Type I timescale of 10^5 yr, and then couple to disk evolution. Subsequently, they migrate inwards on the slow accretion timescale of 10^6 yr, comparable to Type II migration, as predicted by Paardekooper et al. (2010).

Figure 3(b) has some intriguing features that give pause. There is a clear effect of mass on the later evolution of the planets. In the stationary case, the only effect of mass is to determine the speed of migration to the equilibrium radii. In the evolving case, the mass also helps determine the final location of the planet. To show this, we separately plot the tracks of planets of different masses in Figures 3(c)–(e), as well as the trajectories of the equilibrium radii. The planets follow these equilibrium radii until late times, when they decouple.

We can understand the process of decoupling by comparing the viscous accretion timescale to the migration timescale. As the disk thins, the surface density reaches a value so low that the gas cannot transfer sufficient angular momentum to the planet

for its orbital radius to evolve as fast the equilibrium radius. Another way of understanding this is that a perturbation of the planet away from the equilibrium radius will only be corrected if the torque is sufficiently strong to return the planet before the radius moves a substantial distance. As the torque is a function of planet mass, the time and radius when decoupling occurs are also functions of the planet mass.

We can estimate this time and radius by comparing the migration timescale ($t_{\text{mig}} = r_p/|\dot{r}_p|$) to the disk accretion timescale ($t_v = \Sigma/|\dot{\Sigma}|$). As long as $t_{\text{mig}} < t_v$, the planet can keep up with the evolution of the disk. When this is no longer true, decoupling occurs, releasing the planet. We plot the quantity t_{mig}/t_v in Figure 4, for the planet of $1 M_\oplus$ at different times. The structure in the plot comes from the radial derivatives of Σv that define the mass accretion flow, and from the torques Γ that define the migration rate. The spikes in the figure correspond to the equilibrium locations, where $\Gamma = 0$ (and therefore formally $t_{\text{mig}}/t_v = \infty$). The decoupling in Figure 3(d) starts to occur at ≈ 4.0 Myr. In Figure 4, we see that it roughly corresponds to the time when the vicinity of the equilibrium radius crosses the line of $t_{\text{mig}}/t_v = 1$.

Evolution after decoupling proceeds as follows. The inner equilibrium radius corresponds to the inner edge of the isothermal plateau. Once the planet decouples, it is released inside the plateau, itself a region of inward migration since the temperature gradient vanishes. As disk evolution continues, the decoupled planet soon finds itself at the outer edge of the isothermal plateau, and starts migrating outwards. For planets of $1 M_\oplus$, decoupling occurs at $r_p = 1$ AU at 4.5 Myr (Figure 3(b)). The planet then rapidly descends the temperature gradient until it

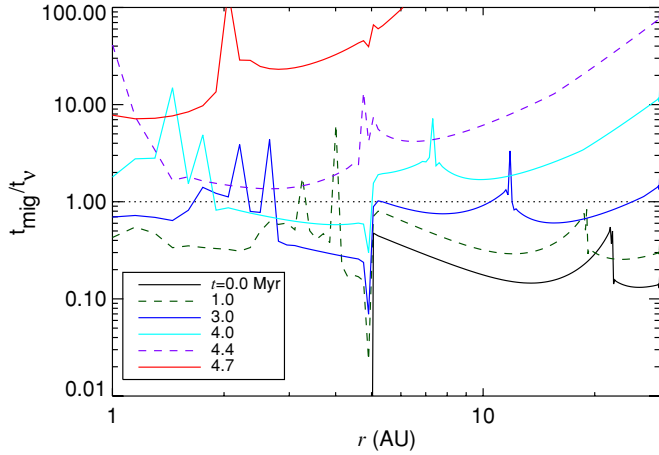


Figure 4. Comparison of the timescales of planet migration (t_{mig}) and disk accretion (t_v) for a planet of $1 M_{\oplus}$.

reaches the outer equilibrium radius. However, this radius too moves inward faster than the planet can migrate, so the planet enters the isothermal outer disk (where $T \simeq T_b$), another region of slow inward migration. At this stage, a planet of $1 M_{\oplus}$ still has time to migrate from $r_p = 2.0$ AU to $r_p = 1.5$ AU before the density drops too low to drive further migration (Figure 3(d)).

The planet of $10 M_{\oplus}$ is strongly coupled and would follow the outer equilibrium radius until it hit the inner boundary of our model at 0.1 AU. The halt at 2 AU seen in Figure 3(e) represents an artificial termination of the simulation. At that point, two criteria had been fulfilled. First, the scale height had become smaller than the Hill radius of the planet, so gap formation should have occurred. This is not sufficient to terminate the simulation, because the inward motion of the equilibrium radius itself occurs at the timescale of Type II migration. However, the second criterion was that the mass parameter determining Type II migration, Σr^2 (Mordasini et al. 2009), had become smaller than the planet’s mass. At this stage, Type II migration becomes planet dominated and we consider that it comes to a halt. The smaller planets never carve gaps.

We investigate migration in disks with different values of \dot{M}_w and \dot{M}_0 , yet constrained by a lifetime of 1–10 Myr, without finding qualitative differences. A change in migration behavior is only seen for hotter disks. For $\alpha_{\text{SS}} = 0.1$, the disks show $\Theta \approx 1$ throughout. Migration then shows a mix of isothermal and adiabatic behavior, being mostly inwards yet with equilibrium points present. The torque only becomes isothermally dominated for $\alpha_{\text{SS}} \simeq 1$, which yields an unrealistically high accretion rate.

4. CONCLUSIONS

In this Letter, we examine the trajectories of planets undergoing Type I migration in evolving, radiative disks with initially nearly adiabatic midplanes, where outward migration can occur. Planets migrate toward equilibrium radii, where the torque acting on them vanishes. These radii correspond to opacity jumps and to the transition, in the outer disk, to an isothermal state. Because of viscous accretion and photoevaporation, these equilibrium radii themselves move inwards on disk accretion timescales.

As long as the torques are strong enough to keep the planets coupled to disk evolution, the planets migrate in lockstep with the gas at the accretion timescale. However, as the disk surface density drops, the timescales of orbital migration and disk accretion eventually become comparable. At this stage, if

the planet is perturbed from an inner equilibrium radius, the equilibrium radius moves inward faster than the torques can return the planet, so it decouples.

If the continuing migration is outwards, the planet encounters another equilibrium radius, and the same process of locking and decoupling occurs. The outermost equilibrium radius lies where the disk reaches the background temperature, and from there the planet can only migrate inwards. However, by the time that the planet decouples even from that equilibrium radius, the disk is already so severely depleted that the ensuing inward migration is feeble, and soon comes to a halt, as the remaining disk mass cannot exert a substantial torque. In no case did a planet released beyond 1 AU migrate all the way to the star.

We stress that we only use a single model for the opacities, which may change as planet formation progresses. The dust size distribution must depend on the balance between coagulation and fragmentation, which remains poorly understood. We also neglect stellar irradiation, which will become important in the late stages of the disk evolution. Irradiation will maintain high temperatures in the inner disk (≈ 100 K; Chambers 2009), preventing gap formation for $10 M_{\oplus}$ planets. On the other hand, irradiation should lead to a hole-forming photoevaporating wind (Clarke et al. 2001; Alexander et al. 2006), which quickly depletes the disk, thus possibly bringing migration to an even earlier halt. Future work should self-consistently address these issues.

As a consequence of the independence of equilibrium radii on planet mass, all planets migrate to these equilibrium locations. Ensembles of planets reaching them may become violently unstable due to N -body interactions. Nevertheless, even if scattered away, migration will invariably drive the planets back toward these radii. The final outcome may well be collisions driving further planet growth, aiding rapid giant planet formation or forming planets in 1:1 resonance.

If this is the case, however, it raises the question of why the solar system has a set of neatly spaced planets as opposed to only two, as the two equilibrium radii of the model might naively suggest. One possible solution is that Γ (and thus any equilibrium radius) shows a dependence on the planet-to-star mass ratio q at the verge of gap opening when $q \approx h^3$ (Masset et al. 2006). Another is that we only consider the fully unsaturated torque, whereas saturation depends on the width of the horseshoe region and therefore on the planet’s mass. However, the level of saturation in radiative disks is not fully understood at present, and we cannot easily add it to our study. Future models should include effects of saturation to study possible mass segregation. Finally, in view of the long migration timescales for $M \lesssim 0.1 M_{\oplus}$, such planets may just not have the time to migrate back to the equilibrium location before the disk vanishes if scattered far enough. This scattered population of small planets could provide the initial conditions for the terrestrial planets of our own solar system.

Our results provide qualitative and quantitative justification for the reduction of Type I migration rates assumed in planetary population synthesis models (e.g., Alibert et al. 2004; Ida & Lin 2008; Mordasini et al. 2009). Instead of migrating on the fast, mass-dependent, timescale t_{mig} , we find that planets spend their first Myr near equilibrium radii that change only on the slow accretion timescale t_v . We show in Figure 4 that $t_{\text{mig}}/t_v \sim 0.1$ for a $1 M_{\oplus}$ planet during most of the evolution of the disk. Examining the same figure for different masses shows a linear dependence on mass, $t_{\text{mig}}/t_v \sim 0.1(M/M_{\oplus})$, consistent with the population synthesis assumptions.

W.L. is partly supported by a Kalbfleisch Research Fellowship from the AMNH. M.-M.M.L. is partly supported by NSF CDI grant AST-0835734, and NASA OSS grant NNX07AI74G. S.J.P. is an STFC postdoctoral fellow. We acknowledge useful discussions with C. Mordasini and T. Birnstiel.

REFERENCES

- Alexander, R. D., Clarke, C. J., & Pringle, J. E. 2006, *MNRAS*, **369**, 229
- Alibert, Y., Mordasini, C., & Benz, W. 2004, *A&A*, **417**, 25
- Baruteau, C., & Masset, F. 2008, *ApJ*, **672**, 1054
- Bate, M. R., Lubow, S. H., Ogilvie, G. I., & Miller, K. A. 2003, *MNRAS*, **341**, 213
- Bell, K. R., Cassen, P. M., Klahr, H. H., & Henning, Th. 1997, *ApJ*, **486**, 372
- Birnstiel, T., Dullemond, C. P., & Brauer, F. 2009, *A&A*, **503**, L5
- Chambers, J. E. 2009, *ApJ*, **705**, 1206
- Clarke, C. J., Gendrin, A., & Sotomayor, M. 2001, *MNRAS*, **328**, 485
- D'Angelo, G., Henning, T., & Kley, W. 2002, *A&A*, **385**, 647
- Goldreich, P., & Tremaine, S. 1979, *ApJ*, **233**, 857
- Hubeny, I. 1990, *ApJ*, **351**, 632
- Ida, S., & Lin, D. N. C. 2008, *ApJ*, **673**, 487
- Kley, W., Bitsch, B., & Klahr, H. 2009, *A&A*, **506**, 971
- Kley, W., & Crida, A. 2008, *A&A*, **487**, L9
- Lin, D. N. C., & Papaloizou, J. 1979, *ApJ*, **309**, 846
- Lynden-Bell, D., & Pringle, J. E. 1974, *MNRAS*, **168**, 603
- Masset, F. S., D'Angelo, G., & Kley, W. 2006, *ApJ*, **652**, 730
- Mordasini, C., Alibert, Y., & Benz, W. 2009, *A&A*, **501**, 1139
- Nakamoto, T., & Nakagawa, Y. 1994, *ApJ*, **421**, 640
- Nelson, R. P., Papaloizou, J. C. B., Masset, F., & Kley, W. 2000, *MNRAS*, **318**, 18
- Paardekooper, S.-J., Baruteau, C., Crida, A., & Kley, W. 2010, *MNRAS*, **401**, 1950
- Paardekooper, S.-J., & Mellema, G. 2006, *A&A*, **459**, L17
- Paardekooper, S.-J., & Papaloizou, J. C. B. 2008, *A&A*, **485**, 877
- Paardekooper, S.-J., & Papaloizou, J. C. B. 2009, *MNRAS*, **394**, 2283
- Papaloizou, J. C. B., & Terquem, C. 1999, *ApJ*, **521**, 823
- Shakura, N. I., & Sunyaev, R. A. 1973, *A&A*, **24**, 337
- Tanaka, H., Takeuchi, T., & Ward, W. R. 2002, *ApJ*, **565**, 1257
- Veras, D., & Armitage, P. J. 2004, *MNRAS*, **347**, 613
- Ward, W. R. 1997, *Icarus*, **126**, 261